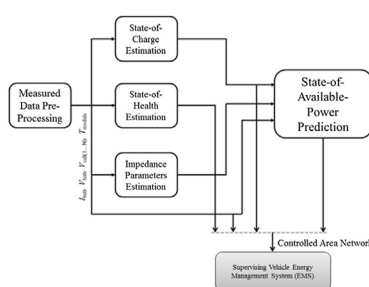Review article

A comprehensive review of on-board State-of-Available-Power prediction techniques for lithium-ion batteries in electric vehicles

Alexander Farmann [a, c, *], Dirk Uwe Sauer [a, b, c]

[a] Electrochemical Energy Conversion and Storage Systems Group, Institute for Power Electronics and Electrical Drives (ISEA), RWTH Aachen University, Germany
[b] Institute for Power Generation and Storage Systems (PGS), E.ON ERC, RWTH Aachen University, Germany
[c] Jülich Aachen Research Alliance, JARA-Energy, Germany

HIGHLIGHTS

- Challenges and issues of on-board SoAP prediction are discussed.
- All available techniques recently applied for SoAP estimation are discussed.
- For every technique the pros and cons of the proposed method are described.
- Examples of existing research results and patents are given.

GRAPHICAL ABSTRACT

ARTICLE INFO

ABSTRACT

This study provides an overview of available techniques for on-board State-of-Available-Power (SoAP) prediction of lithium-ion batteries (LIBs) in electric vehicles. Different approaches dealing with the on-board estimation of battery State-of-Charge (SoC) or State-of-Health (SoH) have been extensively discussed in various researches in the past. However, the topic of SoAP prediction has not been explored comprehensively yet. The prediction of the maximum power that can be applied to the battery by discharging or charging it during acceleration, regenerative braking and gradient climbing is definitely one of the most challenging tasks of battery management systems. In large lithium-ion battery packs because of many factors, such as temperature distribution, cell-to-cell deviations regarding the actual battery impedance or capacity either in initial or aged state, the use of efficient and reliable methods for battery state estimation is required. The available battery power is limited by the safe operating area (SOA), where SOA is defined by battery temperature, current, voltage and SoC. Accurate SoAP prediction allows the energy management system to regulate the power flow of the vehicle more precisely and optimize battery performance and improve its lifetime accordingly. To this end, scientific and technical literature sources are studied and available approaches are reviewed.

1. Introduction

Partial or full electrification of the vehicle powertrains opens a wide range of opportunities to implement more consumer-friendly, security-relevant functions and to discard or reduce the vehicle's

* Corresponding author. Jaegerstr. 17-19, D-52066 Aachen, Germany.
E-mail addresses: alexander.farmann@gmail.com, batteries@isea.rwth-aachen.de (A. Farmann), batteries@isea.rwth-aachen.de (D.U. Sauer).

local emission. In this regard, lithium-ion batteries (LIBs) are favored as promising alternative to other energy storage systems (ESS) such as lead-acid batteries or nickel-metal hydride batteries in automotive applications. In the long term, LIBs are a worthy replacement for fossil fuels and traditional energy sources for use either in mobile or stationary applications [1,2].

High level of gravimetric and volumetric energy and power density, low self-discharge, high cell-voltage (depending on the used active materials) and high cycle and calendar lifetime are among the main advantages of LIBs [3–7]. Considering the growing amount of patent applications of lithium-based technologies from both research institutions and industry in the recent past, a high interest in pushing LIB-based ESS forward can be observed [8].

In order to fulfill specific power and energy requirements in electric vehicles (EVs) generally specified by car manufactures, LIBs are connected in series and/or in parallel (depending on topology), thus forming a large lithium-ion battery pack [9]. The performance of LIBs and their operation are controlled and diagnosed by means of so-called battery management systems (BMS) consisting of both software and hardware [10]. In other words, protection against battery over-voltage, under-voltage, over-current, over-temperature, under-temperature and cell balancing are among the main tasks of the BMS.

Fig. 1 illustrates schematically a simplified lithium-ion battery pack including the following BMS electric and electronic components [11]:

- Cell Controller Board (CCB),
- BMS Master,
- Low-voltage (LV) and high-voltage (HV) interfaces,
- Fuse, contactors etc.

The main task of the CCB is to measure a particular number of cell voltages and temperatures (e.g., 1–12 cells) [11]. In fact, the CCB is the only physical interface between the BMS and the battery cells. Furthermore, cell balancing is performed by means of balancing resistances implemented on each CCB and controlled by an algorithm implemented on the electronic control unit (ECU) in the BMS master. Depending on the topology of the lithium-ion battery pack and the number of LIBs which have to be monitored, one or more CCBs are required. Each CCB communicates with the other CCBs via Controlled Area Network (CAN) or Isolated Communications Interface (isoSPI). Measured cell voltages and temperatures are then submitted via CAN to the BMS Master and analyzed, respectively. On the one hand the BMS Master is responsible for evaluating the measured battery pack's current and voltage as well as triggering the contactors (opening, closing) during pre-charge phases or when a crash or fault is detected, and on the other hand it performs plausibility checks and diagnoses of the battery states and parameters. Furthermore, monitoring algorithms implemented for battery state estimation (BSE) are running on the ECU. Submitting or receiving data to/from the vehicle EMS as well as the electronic power supply are all performed over a designed low-voltage (LV) interface.

The accurate estimation of battery states, such as State-of-Charge (SoC), State-of-Available-Power (SoAP) or State-of-Health (SoH), is still a challenging task, keeping in mind that the implemented monitoring algorithms have to work accurately over years in the particular application. Monitoring algorithms use on-board measured values such as battery temperature, battery voltage and current for BSE. However, since a direct insight into electrochemical processes inside the LIBs in the field is not possible, estimated battery states or parameters may differ from real values. For example, according to Ref. [12], the difference between the measured cell temperature on the surface and in the core may be

approximately 10 K. Keeping in mind that often one single temperature sensor is used in a battery module for monitoring the module's temperature[1] and the measurement accuracy of implemented temperature sensors are often low, it becomes obvious how challenging the task of reliable and accurate battery monitoring is considering all uncertainties and disturbances.

The electrical and thermal performance of the battery is mainly influenced by the following factors:

- Topology of the lithium-ion battery pack [13,16].
- Internal and external factors, such as unequal aging behavior of the LIBs over the battery lifetime (capacity and impedance spread between each individual LIB in the battery module/pack) [9,14],
- Inconsistency of the SoCs [13,15],
- System losses occurring in the battery pack (e.g., power rails, contactor resistances etc.) [9,15],
- Limitation of the use of the battery's maximum power and energy capacity, caused by the increase of battery impedance and decrease of available battery capacity over the battery lifetime [13],
- Distribution of the temperature in the battery pack[2] etc. [7,15].

Therefore, it is necessary to consider these factors during the system design phase in order to prevent oversizing the system and reduce costs, respectively, while specified requirements are fulfilled.

One of the state-of-the-art approaches used for static power capability determination is the hybrid pulse power characterization (HPPC) method presented by the partnership for new generation vehicles (PNGV) battery test manual, published by the Idaho National Engineering & Environmental Laboratory of the U.S. Department of Energy [17]. An improved method for the determination of power capability by means of pulse tests with some modifications regarding applied current rates, resting time etc., is presented in our previous work [18]. In fact, accurate results may be achieved by applying this technique in laboratory environments. But under real conditions, such as in vehicles where available peak current or voltage for a specified time horizon need to be known, accurate power values are not provided and the results are mostly overestimated since only the operational design limit of battery voltage is considered [4,21–23]. Fig. 2 shows the dependence of battery power capability on battery SoC over the battery lifetime at 23 °C in an example of a battery electric vehicle (BEV) prototype using Li(NiMnCo)O$_2$ (NMC)/Li$_4$Ti$_5$O$_{12}$ (LTO) LIBs. The available battery power is determined based on resistance values obtained as a voltage value reached after 20 s from the beginning of the current pulse divided by the current.

The power fade occurred over the battery lifetime directly influences the driving performance of the vehicle in terms of acceleration or battery charging during regenerative phases and charging periods [24]. From the relationship between battery SoC and power capability shown in Fig. 2, it becomes obvious that the charging power capability decreases with the increase of SoC and vice versa. The maximum available power of a lithium-ion battery pack (Fig. 2) is derived by investigating the battery's open-circuit voltage (V_{OCV}) and resistance as follows [25–27]:

$$P_{discharge} = [V_{cell,min} \cdot (V_{OCV\ cell,charge} - V_{cell,min})/R_{cell,discharge}] \cdot n_{cell,series} \cdot n_{module,parallel} \tag{1.1}$$

---

[1] Each battery module consists of several cells connected in series or parallel.
[2] Temperature differences between individual LIBs must be kept in a range of 3 °C–5 °C [19,20].
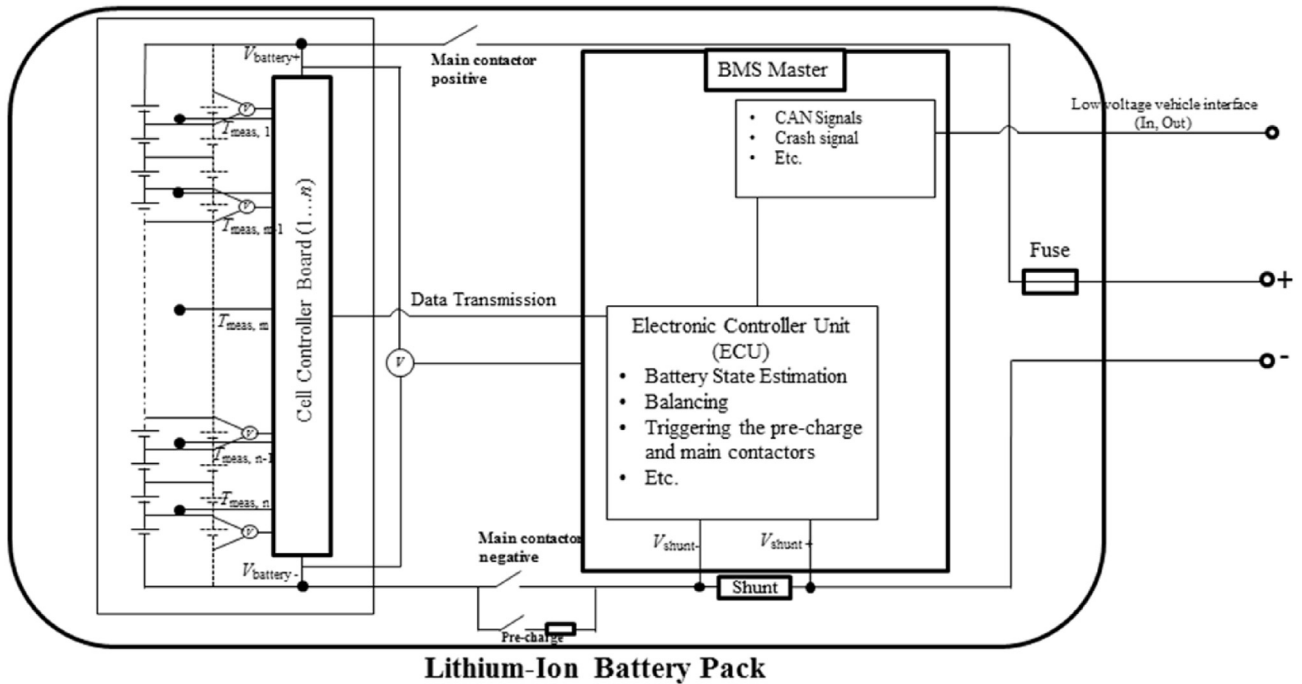
Fig. 1. Schematic illustration of simplified modular-based lithium-ion battery pack including HV/LV interfaces, LIBs, electric and electronic components.

$$P_{charge} = [V_{cell,max} \cdot (V_{cell,max} - V_{OCV\ cell,charge})/R_{cell,charge}] \cdot n_{cell,series} \cdot n_{module,parallel} \tag{1.2}$$

Based on Eqs. (1.1)–(1.2), it can be concluded that the power fade over the battery lifetime is mainly influenced by the increase of battery impedance. The current that can be applied to the battery can simply be derived from Eqs. (1.1)–(1.2) after some mathematical calculations from Ref. [27]. It is worth noting that the applied technique for determination of the battery power capability is independent of the battery chemistry used. However, it is important to ensure the constant battery temperature and to adjust the correct SoC level during the tests.

Generally, as an established rule in automotive applications, the End of Life (EoL) of the battery is reached when its actual capacity has decreased to 70% − 80% of its nominal value or when the impedance has increased up to 100% of its nominal value [25,29]. In Ref. [25], the authors examine the power capability of a battery pack of a BEV at different aging states using three different driving

cycles. The obtained results indicate that when the available battery power fades down to 50% (i.e., the battery impedance is doubled) the vehicle might have trouble accommodating the discharge or charge power at low and at high SoC ranges, respectively. Furthermore, according to the results, the decrease of available battery power leads to the increase of acceleration time, in particular at low SoCs.

The available battery power is limited by the safe operating area (SOA), where the SOA is defined by battery temperature, current, voltage and SoC [30,31]. However, during a single applied current over a time horizon of several seconds ($\Delta t \leq 10$ s), the battery's temperature and SoC do not change significantly. It can be therefore concluded that in practice battery voltage and current are the major limiting factors for SoAP prediction [31,32]. Because of safety reasons the battery must be operated in a specified voltage window ($V_{min} \leq V_{operating} \leq V_{max}$); this limitation influences the maximum current which can be drawn from or fed into the battery and it is therefore often used as an indicator for the battery's power capability. Consequently, the maximum power which is allowed to be applied to the battery can be determined when the pre-defined SOA limit of battery current or battery voltage is reached. It is worth noting that not only the voltage of the lithium-ion battery pack but also the voltage of individual cells must be monitored.

For this reason, by the beginning of the pulse ($t = t_0$), battery voltage and battery current at the end of the applied pulse ($t = t_0 + \Delta t$) should be predicted (Fig. 3).[3] As by the beginning of the pulse it is not known whether the voltage or the current or both of them are limiting factors, one must distinguish between the following four different cases [32,33]:

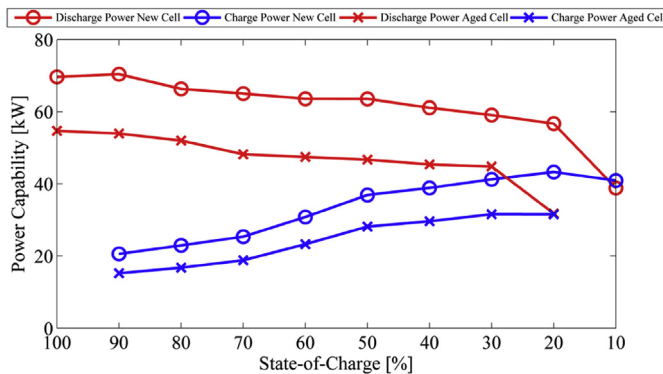- Case A: Charging with cell or battery voltage limitation,

Fig. 2. Power capability of lithium-ion battery pack of BEV prototype using NMC/LTO LIBs ($V_{nominal} = 311$ V, $n_s = 130$, $n_p = 1$, $V_{cell,min} = 1.5$ V, $V_{cell,max} = 2.7$ V) in new and aged states at 23 °C determined as proposed in Eqs. (1.1)–(1.2).

---

[3] Fig. 3 shows cases where it is assumed that constant current pulses are applied to the battery; however, depending on the application, it is also possible that constant power pulses are applied to the battery which means that both the battery current and voltage would change during the applied power pulse.

- Case B: Charging with battery current limitation,
- Case C: Discharging with cell or battery voltage limitation,
- Case D: Discharging with battery current limitation.

In Fig. 3a) and c), the cases are illustrated where the battery voltage at the end of the applied charge or discharge current reaches exactly the allowed upper or lower voltage limit (see case A and case C above). In these two cases the predefined current limit is not exceeded. At the same time in Fig. 3b) and d), the maximum limiting charge and discharge current is applied to the battery while the upper or lower voltage limit is not reached (see case B and case D above). In fact, case B is the only case among all the four listed cases where the battery is charged with the maximum limiting current while the absolute value of the available battery power is increasing. In the remaining cases, the absolute value of the available battery power decreases over particular charging or discharging periods.

As a general rule, the time horizon for SoAP prediction lies between 1 s and 20 s in BEVs and hybrid electric vehicles (HEVs) [10]. By knowing the available battery power in addition to the actual battery SoC and SoH, a reasonable EMS strategy can be applied and specified vehicle functions, such as vehicle acceleration, deceleration or gradient climbing can be performed without exiting battery SOA and affecting the lifetime of the battery or causing safety damage, respectively [26,34,35].

In addition to the discussed impacts of battery SoC, current and voltage on available battery power, it is essential not to neglect the influence of battery temperature. Since applied high charge or discharge current rates or battery temperatures may influence the aging behavior of the battery (e.g., lithium plating[4] etc.) [36], the SoAP prediction algorithm must consider these boundary conditions as well. Fig. 4 shows the dependence of SoAP on temperature and applied current rate in an example of a BEV prototype using NMC/LTO LIBs. As expected, the available battery power for both charge and discharge direction decreases with the decrease of battery temperature, as a consequence of increasing battery resistance. At the same time, the available battery power increases with the increase of temperature while aging processes occurring in the LIB are faster under such operating conditions.

This study aims to give an overview of available techniques for SoAP prediction of LIBs in EVs. Unfortunately, it seems that there is no uniform definition available in the literature for battery power capability. The definition used in this study, namely SoAP, differs little from the definition of State-of-Function (SoF) estimation which is often employed. SoF is a figure of merit that describes the battery capability to perform a certain task [38,39]. In the particular case of battery power capability, it may be concluded that SoF is a kind of logical signal that only allows yes or no response to the required battery power for a certain function, such as cranking capability etc. At the same time, SoAP is mainly related to the amount of power which the battery can deliver to or accept from the vehicle powertrain over a certain time horizon (Δt) [19,40–42]. Therefore, in order to prevent misinterpreting of the used parameters, in this study we will only use the SoAP definition whose meaning and particular definition is described above. An alternative definition is given in Refs. [43,44], where the authors state that SoAP is actually defined as a ratio of available battery power to the maximum nominal battery power.

Up to now, different approaches for SoC and SoH estimation of LIBs have been shown and reviewed in the literature by many authors in the past. However, the topic of SoAP prediction has not

been explored enough sufficiently yet and there are still a lot of researches required to optimize, improve and understand this challenging task. In this context, the available techniques for predicting the SoAP can generally be subdivided into the following two groups:

- Methods based on (adaptive) characteristic maps (CMs),
- Methods based on equivalent circuit models (ECMs).

In the following sections, the methods for SoAP prediction discussed in scientific and technical literatures are reviewed. It is worth noting that the focus is not to describe each individual method in detail, but rather the elaboration of the strengths and weaknesses of the respective technique. The remainder of this article is organized as follows (Fig. 5): In Section 2, techniques based on adaptive characteristic maps are introduced and discussed. Estimation techniques based on ECMs and corresponding literature are reviewed in Section 3. Finally, this work is summarized in the conclusion.

2. Methods based on (adaptive) characteristic maps

The methods based on characteristic maps (CM) use the known static interdependences between battery power capability and battery parameters and states. Related battery parameters and states generally used in this context are listed as follows [45,46]:

- SoC,
- Temperature,
- Duration of the power pulse,
- Required power,
- Battery voltage.

In order to build the CM: First, the above mentioned dependences are characterized by various battery characterization techniques, such as HPPC tests or electrochemical impedance spectroscopy (EIS). Second, the extracted parameters are stored as a more dimensional matrix in a non-volatile memory in the ECU used as initial parameter sets of the battery.

As discussed in the previous section, because of aging mechanisms occurring in the LIBs, their impedance characteristics change over the battery lifetime. This makes the use of adaptive techniques for tracking the CMs over the battery lifetime necessary. The basic idea of the techniques using CMs is simple: The battery power measured on-board is compared with the predicted value ($\Delta P = P_{\mathrm{meas}} - P_{\mathrm{estim}}$) and the corresponding reference point in the CM is adapted if a deviation between both values is detected. This process yields more accurate future power prediction in the corresponding area of the map.

Among the main advantages of CM-based techniques for predicting the SoAP are its simple implementation and straight forward characteristic. However, since batteries are nonlinear devices, there are some issues which need to be considered thoroughly. First, battery's characteristics (e.g., dynamic behavior etc.) depend strongly on its previous history. Various electrochemical processes, such as charge transfer processes become pronounced when dynamic load is applied to the battery. Since these effects are not considered in the CMs, the SoAP prediction accuracy is significantly affected. Second, the dependences of the above mentioned parameters are stored on the memory in multidimensional form. This means that a high amount of storage capacity is needed depending on the amount of parameters. Unfortunately, in most cases, data storage capability and computational resources on microcontrollers are limited. Therefore, a specific functional extension is required in order to reduce the computational effort, so that the dependences

---

[4] Lithium plating refers to deposition of metallic lithium in form of dendrites in the anode [37].
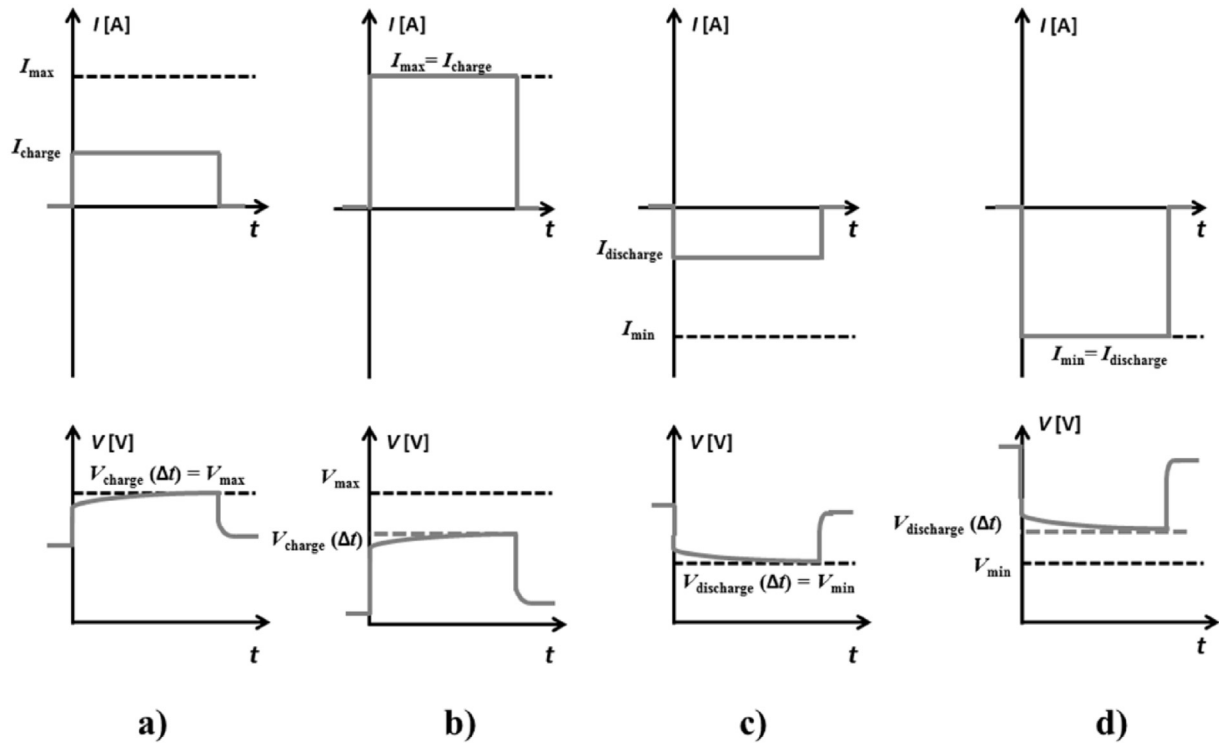
Fig. 3. Schematic illustration of four cases for limiting available battery power in case of battery charging or discharging with constant current: a) applying constant charge current ($I_{charge} < I_{max}$) while battery voltage is the limiting factor (in this case the battery could be at very high SoC range); b) applying constant charge current ($I_{charge} = I_{max}$) while current is the limiting factor ($SoC_{case,b} < SoC_{case,a}$); c) applying constant discharge current ($I_{discharge} > I_{min}$) while battery voltage is the limiting factor (in this case the battery could be at very low SoC range); d) applying constant discharge current ($I_{discharge} = I_{min}$) while current is the limiting factor ($SoC_{case,d} > SoC_{case,c}$).
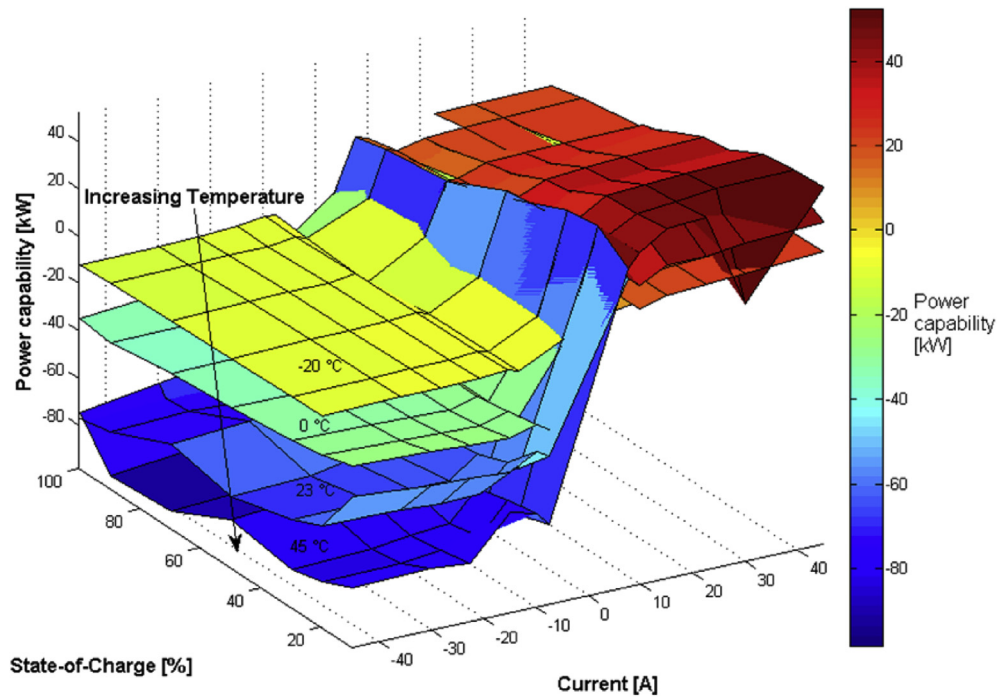
Fig. 4. Dependence of available battery power on battery current and SoC at different temperatures in an example of a lithium-ion battery pack prototype using NMC/LTO LIBs in new state ($V_{nominal} = 311$ V, $n_s = 130$, $n_p = 1$, $V_{cell,min} = 1.5$ V, $V_{cell,max} = 2.7$ V) determined as proposed in Eqs. (1.1)–(1.2).

of the parameters are approximated by empirical functions (e.g., polynomial functions) [33,47–49].

In Ref. [45], the authors present an adaptive CM-based (ACM) technique where the dependences between actual SoC, temperature, duration of the applied load (1 s–10 s) and available power of LIBs are considered. Moreover, battery voltage and current are

measured and observed over a pre-defined time horizon and consequently compared with a reference power value of the CM. If any difference is detected and it is higher than a value specified beforehand, the respective reference point of the CM is adapted accordingly.

In Ref. [47], a method for determining the maximum available charge or discharge battery power depending on actual battery SoC, temperature and its actual aging state (available discharge capacity) is discussed. A 5th order polynomial function is applied in order to build the interrelation function between power and SoC and between power and available discharge capacity. The interrelation function between temperature and power is built by means of a 2nd order polynomial function.

In Refs. [48,49] a self-learning technique for SoAP prediction in HEVs as an example of NiMH and Lead-Acid batteries is introduced. The authors introduce an algorithm employing ACM where the 2nd order polynomial function is used to approximate the operating point of the CM by means of simple multidimensional regression techniques, resulting in less consumption of the memory on the microcontroller. Otherwise, according to the authors, about 3000 measured values would have to be stored which requires a high amount of memory capacity. In this context, the battery behavior is represented by the coefficients of the used polynomial function. In order to track the battery's characteristics over its lifetime, the applied regression function is continuously updated during operation. The dependences between voltage, SoC, temperature, pulse duration and the absolute power value are employed to build the ACM. The implemented algorithm is able to predict the SoAP under the above conditions by considering the allowed voltage window.

In Ref. [50], an algorithm for estimating certain parameters such as battery discharge power, available charge capacity, overcharge or over discharge detection of lithium-ion battery packs in HEVs is presented. For this reason, the authors propose to use the determined battery internal resistance as a reference for estimating the above mentioned battery parameters. In this regard, the proposed algorithm uses the values of internal resistance and OCV for a given SoC from CM and determines the available battery power based on Eqs. (1.1)–(1.2). However, the non-adaptive nature of the proposed algorithm and neglect of the influence of temperature are its main disadvantages. Consequently, the values of the internal resistance remain constant over the battery lifetime although an increase of battery resistance during operation is expected.

3. Methods based on equivalent circuit models

As a second technique for predicting the battery SoAP, model-based methods employing ECMs are discussed in this section. These techniques differ mainly in the used ECM and methodology for on-board parameters and battery states identification. In order to be able to predict the available battery power accurately, it is necessary to use a dynamic battery model which reproduces electrochemical processes occurring in the battery as accurately as possible. However, a feasible replica of each of the processes can rarely be obtained since up to now many processes occurring under different conditions are not identified or understood sufficiently. In this regard, physics-based electrochemical battery models considering spatially distributed behavior of the battery states are the most promising solution for comprehensive battery analysis. In fact, because of their high complexity and the required high computational effort, such battery models are not suitable for BSE. In this context, it may be stated that model-based approaches using simple electrical models are the most promising solutions for estimating the available battery power in BEVs or HEVs where high dynamic loads are present.

A simple impedance-based ECM describing the electrode reactions in the ESS was first proposed by Randle in Ref. [51]. The proposed ECM consisting of resistances (including ohmic and charge transfer resistance) and a double-layer capacitance is still very popular in BMS applications, mainly because of its simplicity. Since then, many other more complex ECMs representing various electrochemical processes in great detail have been proposed by other researchers. Reviews and descriptions of different impedance-based battery models may be found in Refs. [52–55].

Considering the limited computational power of BMS, reducing the model parameters to a minimum by trying to depict the electrochemical processes as accurately as possible becomes necessary. In this regard, ECMs employed in the BMS often consist of a V_{OCV}, a simple linear ohmic resistance and a number of RC-elements connected in series. The number of applied RC-elements depends highly on the application, relevant time constants and required estimation accuracy. A higher number of RC-elements leads to higher estimation accuracy while at the same time the computational effort increases [29,56–58]. An example of a possible ECM for integration in a BSE algorithm is shown in Fig. 6. Each element of the ECM refers to a certain electrochemical process during battery operation or even in a battery steady state. R_0 refers to the resistance contribution of electrolyte, battery poles, corrosion, conductors. RC-elements reproduce polarization overvoltages that mainly occur because of passivation layers on the electrodes, charge transfer processes at the interfacial between electrode and electrolyte, diffusion, migration and remaining convection processes. The open-circuit behavior of the battery is represented by means of a V_{OCV}.

In an example of the ECM shown in Fig. 6, the estimated battery voltage $V_{estim}(\Delta t)$ at the end of the (dis)charging current pulse for a certain time horizon of Δt can be derived as follows:

$$\Delta V_{R0} = R_0 \cdot I \tag{3-1}$$

$$\Delta V_1(\Delta t) = V_1(t=0) \cdot e^{\frac{-\Delta t}{R_1 C_1}} + R_1 \cdot \left(1 - e^{\frac{-\Delta t}{R_1 C_1}}\right) \cdot I \tag{3-2}$$

Section 2
Methods based on Adaptive Characteristic Maps

Section 3
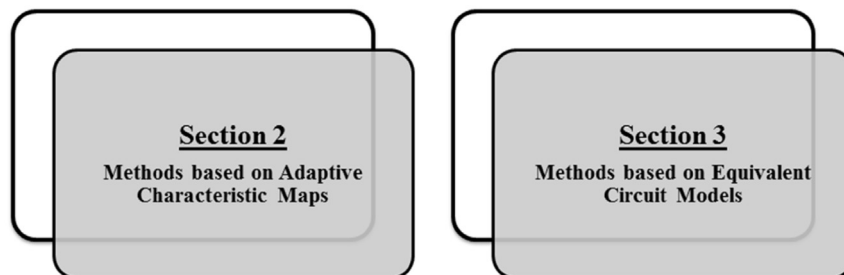**Methods based on Equivalent Circuit Models**

Fig. 5. Organization of the present paper.

$$\Delta V_2(\Delta t) = V_2(t=0) \cdot e^{\frac{-\Delta t}{R_2 C_2}} + R_2 \cdot \left(1 - e^{\frac{-\Delta t}{R_2 C_2}}\right) \cdot I \tag{3-3}$$

$$\Delta V_n(\Delta t) = V_n(t=0) \cdot e^{\frac{-\Delta t}{R_n C_n}} + R_n \cdot \left(1 - e^{\frac{-\Delta t}{R_n C_n}}\right) \cdot I \tag{3-4}$$

$$V_{estim}(\Delta t) = \Delta V_{R0} + \Delta V_1(\Delta t) + \Delta V_2(\Delta t) + \Delta V_n(\Delta t) + V_{OCV}(SoC) + \upsilon(SoC) \cdot \Delta t \cdot I \tag{3-5}$$

where $\upsilon(SoC)$ [V·A^{-1}·s^{-1}] represents the change of the V_{OCV} per As of current flow.

In Ref. [57] a wide overview of ECMs that are often applied for BSE in BMS for automotive applications is given. Employed ECMs are compared considering their robustness, model complexity and accuracy of the estimated battery voltage. A multi-swarm particle algorithm is employed for estimating the ECM parameters on-board. On the one hand, using a complex ECM yields a higher degree of voltage estimation accuracy, but on the other hand the parameter identification of such ECMs requires high computational power which is rarely given on a microcontroller. In our previous work [59], the applicability of enhanced ECMs using two ZARC-elements for on-board voltage estimation in BMS is introduced. The ZARC-elements corresponding to different electrochemical processes are approximated by means of odd number of RC-elements, where the ECM parameters are identified using the enhanced varied parameter approach technique. The presented ECM is much more accurate for battery voltage estimation in comparison to other commonly used ECMs, such as ECMs using one or two RC-elements.

In order to ensure high estimation accuracy over the battery lifetime and under various operating conditions (e.g., various temperatures and SoCs), ECM parameters need to be adapted to the actual aging state of the LIB on-board [60]. In Ref. [14], the authors show that the estimation accuracy could decrease over the battery lifetime even if the parameters of the ECM are adapted to the actual aging state of the battery. Algorithms presented in many researches in the past were often validated under nominal conditions or when the battery was in a new state. However, as discussed in Refs. [30,32], the accurate prediction of the available battery power becomes more challenging at low temperatures or when the battery is aged, as the LIB reaches the predefined SOA and power limits, respectively, readily.

As a common solution for ECM parameters estimation, the battery model is represented in a discrete-time state-space form. The methods differ in the way how the states and parameters of the model are estimated. Generally, it can be differentiated between the following two techniques [29,61]:

- Adaptive joint estimation technique,
- Adaptive dual estimation technique.

With the joint estimation technique an adaptive filter is applied on a single vector of unknown parameters and states for their estimation. The dual estimation technique uses two filters in parallel. One filter is used for the state estimation and the other one for the parameter estimation. A selection of well-known methodologies that are often applied for the on-board estimation of the ECM parameters is listed in Fig. 7.

The first two techniques, namely Kalman filter-based (KF) and Least-Square-based (LS) estimators, belong definitely to the most often employed recursive estimators in various engineering disciplines. In both cases, the system uses a linear regression model in a generic form [62,63]. Algorithms based on the KF technique are widely spread in the field of BSE. KF was for the first time presented in 1960 by Kalman in Ref. [64]. However, since KF can only be applied to linear systems and batteries show a highly nonlinear behavior (e.g., current dependence of the charge transfer resistance etc.), it is often used in combination with other extended filters (e.g., Least-square, Extended Kalman filter (EKF), Sigma-Point Kalman filter (SPKF) etc.).

There are some disadvantages of the KF-based algorithms which need to be addressed: a) required complicated matrix calculations (i.e., Jacobian matrix), b) the linearization of the nonlinearity of the battery characteristics and the necessity of knowing a priori the variable of the system noises, such as mean value, relevance and covariance matrix. An inconvenient information matrix of the system noise may yield estimation error and parameters divergence, respectively [65–67].

3.1. Kalman filter-based methods

In Ref. [40], a SoAP prediction technique using KF for estimating ECM parameters (*R-RC*) is introduced. The main differences with regard to the definitions of SoF and SoAP are carefully addressed and alternative possibilities are provided. The applied algorithm considers the change of V_{OCV} during the applied discharge current pulse ($dV_{OCV}/dI \cdot \Delta t$) which consequently improves the V_{OCV} convergence and estimation accuracy of the algorithm. For verification reasons, HPPC tests and urban dynamometer driving schedule (UDDS) load profile are used. Eqs. (1.1)–(1.2) are employed as a basis for SoAP prediction where battery non-linearities are neglected and only the discharging case is considered.

In Ref. [68], the authors present an approach based on a KF filter for SoAP prediction in an example of lead-acid battery. An ECM (*R-RC*) considering the nonlinearity of charge transfer processes by means of the Butler-Volmer equation (BVE) is applied and the results are compared with the same model neglecting the mentioned nonlinearity. After analyzing the results, the authors state that considering the aforementioned nonlinearity improves the estimation accuracy significantly. However, there are some points which may be addressed here: First, the symmetry coefficient is assumed to be equal for both anodic and cathodic reactions (i.e., $\alpha = 0.5$) in this work, which is actually not applicable to lead-acid batteries and could at best be applied to LIBs [66,69]. Second, for both models the exchange current density is assumed to be constant. In fact, the exchange current density decreases over the battery lifetime and is highly temperature-dependent as shown in our previous work [18]. This means that the accuracy of the proposed algorithm might decrease over the battery lifetime. Real vehicle data gathered in the field are used to verify the algorithm whereas the SoAP estimator is only validated for cases when maximum allowable discharge current is drawn. Furthermore, in Ref. [70], the same authors investigate the Arrhenius equation and consider temperature as model input for the determination of resistance and overvoltage in an example of LIBs using LFP cathode. Based on the KF technique, parameters of the ECM are identified on-board. In contrast to the previous work, the temperature dependence of the ECM parameters is considered in the model. Obtained results indicate the necessity of considering the nonlinearity at very low temperatures while a significant improvement with regard to the voltage prediction accuracy could be achieved.

In Ref. [71], an approach based on *R-RC* ECM for predicting the battery's SoAP is presented. Battery current and voltage are considered as limiting factors for the applied algorithm. As an advantage, in the employed algorithm the difference between each individual cell V_{OCV} is considered to identify the weakest cell in the
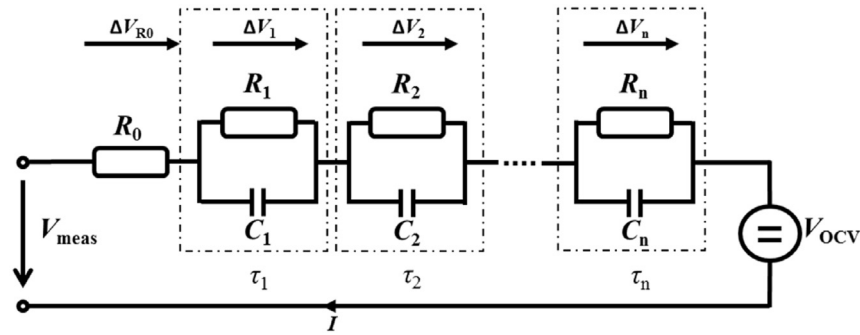
Fig. 6. An example of an equivalent circuit model employed in battery management systems considering various time constants.

battery pack. V_{OCV} is determined based on a nonlinear SoC-OCV correlation characterized in the laboratory. Evaluating each cell's V_{OCV} by its own has on the one hand the advantage that the weakest LIB (LIB with minimum V_{OCV} for discharging case or LIB with maximum V_{OCV} for charging case) in the battery pack can thus be simply identified, but it requires on the other hand a higher computational effort since in large lithium-ion battery packs often large amounts of LIBs are connected in series and each LIB have to be supervised individually. In this regard, the authors propose using only the information from maximum V_{OCV} in case of charging and minimum V_{OCV} in case of discharging. Unfortunately, no information has been provided with regard to the estimation technique applied for impedance parameters; the authors mention, however, that KF-based algorithms could be applied.

In Ref. [78], a novel algorithm for SoAP prediction is proposed where an impedance-based ECM using the Warburg impedance connected in series with a simple *R-RC* circuit is employed. An adaptive approach based on fractional joint KF is applied for on-board impedance parameters and SoAP estimation. Unfortunately, the RC-element representing the charge transfer processes is neglected and thereafter it is simplified to a linear resistance. The authors define SoC, *I* and *V* for both charge and discharge cases as limiting factors for the SoAP prediction algorithm. For verification reasons, constant current pulses with durations of 10 s and 60 s are inserted to the FUDS load profile and the predicted SoAP at the end of the pulse is analyzed. As discussed beforehand, such algorithms may work accurately and robust under the nominal condition described by the authors but it is definitely of interest to examine the applied technique under conditions beyond nominal.

3.1.1. (Dual) extended Kalman filter-based methods

In the system theory, EKF is widely used for the state estimation of nonlinear systems where at each time step a linearization process of the system by means of a linear time-varying (LTV) system is performed. It is assumed that the noise processes are zero mean white Gaussian stochastic processes of covariance matrices which refer to the uncertainty of the state estimation. As a main difference to the KF algorithm, battery nonlinearities (nonlinear state transition function and nonlinear measurement function) are approximated by means of first-order Taylor-series expansions at each time step [61,72]. In this context, different approaches using EKF as joint or dual estimator for SoAP predictions are discussed in great detail in Refs. [73,74].

In Ref. [73], a model-based approach using EKF for estimating impedance parameters, voltage across the RC-element and SoAP prediction in an example of a HEV is presented. Minimum charging current or maximum discharging current for ($\Delta t = 1-10$ s) is determined after performing some simple mathematical calculations from the employed ECM (*R-RC*). Based on the derived limiting current values, (dis)charge voltages of the battery pack are calculated for the desired time horizon. The proposed algorithm is verified under nominal conditions in a Model-in-the-Loop (MIL) environment.

Furthermore, in Ref. [74], an EKF-based algorithm for on-board impedance parameters estimation is proposed where pre-defined limits for ECM-parameters depending on battery temperature
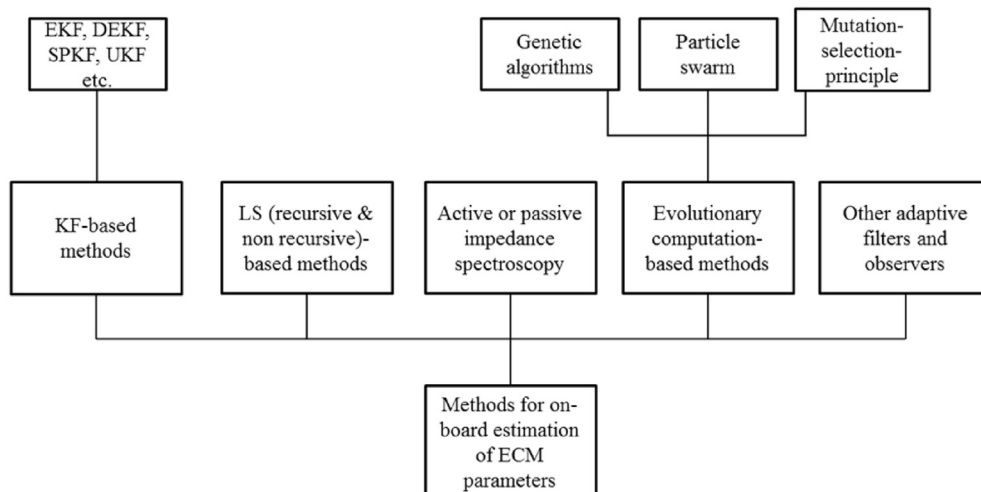

Fig. 7. A selection of commonly applied techniques for ECM parameters estimation.

and SoC are set. A simple *R-RC* ECM is employed where the correct and meaningful convergence of the impedance parameters is ensured by setting the upper and lower limits of the impedance parameters. Moreover, in Ref. [75] the authors present a novel technique for estimating the impedance parameters of the ECM and instantaneous SoAP prediction. The parameters of the lithium-ion battery pack used in a HEV are extracted by means of EIS measurements for an initial state. Based on various filters, such as high-pass, low-pass or band-pass filters and/or a combination thereof, the measured battery's voltage response is split up into different appropriate frequency ranges (medium to high frequency range as well as low and steady-state part). When the impedance parameters of the ECM for the respective frequency range are identified, the battery's limiting current and instantaneous power can then be simply determined. The authors propose an EKF-based algorithm for estimating the parameters of the RC-element on-board. However, since the corresponding frequencies are influenced by many factors such as temperature and actual aging state of the battery, the impedance parameters estimation from each frequency range might be underlined some inaccuracies when the battery is operated under conditions other than those initially obtained. In addition, since commercially available hardware for performing EIS-measurement in the vehicles is still in a primitive development stage, accurate measurements over a wide frequency range can hardly be carried out.

In contrast to the above referenced literatures where adaptive joint estimators using EKF for SoAP prediction are proposed, in Refs. [23,44], the authors propose a SoAP estimation technique based on the dual extended Kalman filter (DEKF). The DEKF method uses two EKFs (i.e., a Kalman state and a weight filter) that run concurrently at every time step, where one filter is responsible for state estimation (e.g., SoC or SoAP etc.) and the other one for parameters identification (e.g., R_0, τ, R_{ct} etc.) while both of them concurrently provide each other with derived information and ensure a more stable independent estimation path in this way.

In Ref. [44], an *R-RC* ECM using the DEKF algorithm for on-board parameters estimation is used, where battery current and voltage are considered as limiting constraints for SoAP estimation. Each of the limiting factors (current and voltage) is considered separately and its impact on SoAP is discussed thoroughly. For the applied DEKF algorithm, the flowing current through the charge transfer resistance is taken into the state vector, and the remaining parameters of the ECM (R_0, τ, R_{ct}, V_{OCV}) with a slower rate of change are stored in the parameter vector. The proposed algorithm is examined by performing verification experiments on the LIBs using LFP cathode at different aging states and temperatures. For verification reasons the FUDS load profile is used as a reference. Furthermore, the maximum time that the current can be applied to the battery and voltage limits is determined based on an ECM employed. Unfortunately, during verification tests a narrow range of applied current ($-3C - +2C$) is examined. According to the authors, promising results for SoAP prediction with a relative estimation error of less than 5% could be achieved. However, the proposed technique neglects the battery nonlinearities and no SoAP prediction results for a particular time horizon are provided. In fact as discussed in Ref. [59], the impact of the applied current-rate on the voltage estimation accuracy is not negligible; therefore, higher current rates which actually often occur in a real field must be considered. Moreover, the obtained results indicate the decrease of voltage estimation accuracy at very low SoC range, which occurs mainly because of high pronounced diffusion processes [30].

Furthermore, in Ref. [26] the authors propose a static SoAP prediction (using SoC-R_i relationship) methodology based on the EKF technique (EKF is employed for SoC estimation). An *R-RC* ECM

with a little deviation concerning the internal resistance is implemented. The instantaneous available battery power is derived based on Eqs. (1.1)–(1.2). The authors combine the ohmic and charge transfer resistance in one linear resistance connected in series with the RC-element representing diffusion overvoltage. The combination of both resistances may help to overcome the mentioned linearization problem of battery's nonlinear characteristics by EKF algorithms. However, since the impedance parameters change over the battery lifetime, it is essential to ensure their adaption to the actual battery aging state.

In Refs. [23,28,76], battery voltage, current and SoC limits are considered as constraints for SoAP prediction in a lithium-ion battery pack. In Ref. [23], the possibility to employ EKF and DEKF methods for impedance parameters and SoC estimation of LFP-based LIBs is discussed comprehensively. Moreover, in Refs. [28,76], maximum discharge and minimum charge currents are determined based on derived battery SoC and resistance values. Two algorithms are proposed for SoAP prediction and their performances are compared, where simple ECMs employing a simple ohmic resistance connected in series with V_{OCV} are implemented and the available battery power is determined based on Eqs. (1.1)–(1.2). In order to be able to predict the available battery current for a specific time horizon (Δt), the change of V_{OCV} over the prediction time horizon is estimated by means of the Taylor-series expansion. In the second algorithm proposed, the ECM is implemented in a state-space form and the limiting battery current considering the voltage and SoC limits is estimated based on the bisection search method. However, in both cases the employed ECMs are very simple and neglect battery nonlinearities and polarization effects. Moreover, the available battery power is determined separately for individual LIBs in the battery pack; this fact requires high computational power that is actually not given on commercial microcontrollers used in the automotive industry.

In comparison to the described EKF techniques, the adaptive extended Kalman filter (AEKF) improves the estimation accuracy by an adaptive update of the noise covariance. In this regard, several studies have investigated AEKF for SoAP prediction. In Ref. [77], an adaptive joint estimator employing a simple *R-RC* ECM for SoC and SoAP estimation is presented. LIBs using LFP cathode at various temperatures and aging states are investigated. The Nernst model is used to build and adapt the nonlinear SoC-OCV correlation over the battery lifetime and make the SoC be a part of the developing model, respectively. Battery SoC and SoAP are estimated by means of AEKF where the UDDS load profile is used as a reference for verification reasons. Moreover, a simple LS estimator is used to identify the ECM parameters. In addition to the estimated SoC, the battery's design limits, namely voltage and current, are defined as constraints in the implemented SoAP estimator. The available battery power is determined and validated for $\Delta t = 0$ and $\Delta t = 30$ s. Since current and voltage limits for the respective operating condition and the battery's aging state are calculated on-board, safety damaging the LIBs by either over- or underestimating the available power can be prevented. However, for verification tests, the applied current is downscaled to ± 2 C, which is actually low (especially in case of HEVs) as mentioned above and might influence the reliability analysis of the proposed algorithm.

Furthermore, in Ref. [65] the authors present an AEKF-based six-step joint estimator for SoC and SoAP estimation (verified for $\Delta t = 15$ s, 30 s, 60 s) in an example of plug-in hybrid electric vehicle (PHEV). An *R-RC* ECM is applied, where HPPC tests and UDDS load profiles are applied in order to verify the robustness and real-time applicability of the proposed algorithm. However, since the authors use the Nernst equation to build the nonlinear SoC-OCV correlation and the limiting battery current is determined based on the actual battery's SoC, the estimation accuracy of the model might decrease

over the battery lifetime or when the operating temperature differs extremely from the one used to parameterize the Nernst equation.

In Ref. [34], the authors present a multi-states joint estimator employing the recursive least square technique with optimal forgetting factor (RLSF) for impedance parameters estimation and an AEKF for SoC and SoAP estimation. In addition, battery voltage, current and SoC are considered as limiting factors for the SoAP prediction algorithm. LIBs using LFP cathode at various aging states are used for verification reasons and an R-RC ECM is employed, where the ohmic resistance is implemented separately for charge and discharge directions. Thus, in total there are four impedance parameters needed to be identified on-board. The identified parameters are transmitted to the prior state estimator in order to update the battery's SoC. Since the SoC-OCV correlation is built by the Nernst equation, the V_{OCV} is then updated over the equation when new SoC values are available. Thereafter, the battery's SoAP is predicted based on the results from the SoC and parameter identification estimators. According to the authors, promising results for SoAP prediction with a relative estimation error of less than 1% could be achieved.

3.2. Least-square-based methods

As alternative popular technique for on-board impedance parameters and state estimation, the algorithms based on the least square (LS) technique are widely used in BMS applications. The required computational effort for LS-based algorithms is low and the respective algorithms can simply be implemented on the microcontroller. The underlying idea of LS-based algorithms is very simple; it is mainly based on the minimization of the sum of squared prediction errors. The LS-based filters consider input data, model states and parameters as deterministic signals. Among the main disadvantages of LS-based algorithms are their divergence problem and the fact that they are not suitable for application on very complex ECMs. There are different classifications of LS-based filters known for time varying parameters estimation, such as recursive least square (RLS), recursive extended least square (RELS), least square with forgetting factor, weighted least square (WLS), weighted recursive least square (WRLS) etc. [79].

3.2.1. Recursive least-square-based methods

In Ref. [84] the authors show the results of the applied SoAP and voltage estimator by performing verification tests on the test bench and in HEV. The obtained results of the predicted voltage indicate an estimation accuracy of approx. 5% where the impedance parameters of the ECM are identified by means of the simple RLS algorithm, and a predictive control algorithm based on step response, so-called Dynamic Matrix Control (DMC), is employed for the maximum discharge current estimation. The applied DMC algorithm belongs to the class of filters employed in the systems theory which is able to determine a sequence of manipulated variables for predicting the upcoming behavior of the model. The main important difference to the previously discussed literature lies in the applied ECM, where n RC-elements are connected in series and the time constant of each RC-element is determined offline. However, the developed algorithm is only evaluated for the discharging case whereas the charging case (e.g., regenerative braking etc.) is neglected.

A novel approach for SoAP prediction considering both voltage and current as limiting factors is presented in Ref. [80]. Within this approach, a so-called moving average (MA) noise covering the remaining battery overvoltages (e.g., diffusion processes etc.) is connected in series with RC-element and ohmic resistance in the ECM. Furthermore, an RELS algorithm is applied for impedance parameters identification. The main advantage of the RELS

algorithm over the common RLS algorithm is the additional implementation of a feedback process which allows the estimate of unmeasurable noise. The proposed algorithm is validated by UDDS load profile and HPPC tests while the algorithm's accuracy is analyzed for various time horizons (5 s − 120 s). The achieved results indicate a more accurate and reliable SoAP prediction by employing the proposed ECM rather than a simple R-RC model, especially for cases where the SoAP is predicted for a large prediction time horizon. As the next step, the presented approach might be investigated in more detail under real conditions and especially over a wide temperature range since it is only validated under nominal condition.

In Ref. [4] the authors propose an algorithm for SoAP prediction considering SoC, current and voltage as limiting factors. A RLS-based technique with optimal forgetting factor (RLSF) is applied to estimate battery impedance parameters. The main difference of the proposed technique (RLSF) in comparison to the common RLS filter is that if the model parameters change continuously but slowly, the RLS technique is rarely able to capture the occurred changes instantaneously. Therefore, an enhanced filter is required, which gives more weight to recent data than to an older dataset as proposed in Ref. [34]. The on-board applicability of the proposed algorithm is then verified by means of hardware-in-the-loop (HIL) tests using the FUDS load profile as a reference. A simple R-RC ECM is employed where the V_{OCV} is modeled by Nernst model. Moreover, the change of the V_{OCV} over a prediction time horizon is determined, which leads to higher voltage prediction accuracy. According to the authors, promising results could be achieved with the battery voltage estimated within an accuracy range of 1%.

In Ref. [27], the authors investigate a method for SoAP prediction in an example of a transporter, the so-called Segway. Based on Eqs. (1.1)–(1.2) presented in Section 1, the available battery power is simply determined. The authors propose using LS or RLS-based techniques for estimating the battery resistance and V_{OCV}. Furthermore, based on the estimated values for available battery power, the maximum velocity of the transporter is determined. In this particular case it is assumed that the current is equal to the electric-motor current and the resistance is determined as a sum of the motor winding resistance and battery resistance.

In addition to the methods discussed above, in Refs. [32,85], the authors present an adaptive technique for SoAP prediction of the lithium-ion battery pack using the varied parameters approach (presented in Ref. [66]) for impedance parameters estimation. The current dependence of the R_{ct} is considered in the proposed algorithm by simplifying the BVE. The authors employ a nonlinear R-RC ECM where the differences between SoCs and resistances of individual LIBs are considered in an implicit way. Battery voltage, current and SoC are considered as limiting factors for SoAP prediction. In order to identify the weakest LIB in the battery pack, V_{OCV} and resistance are considered as supporting indices. In this regard, the LIB with the highest V_{OCV} for charging case or lowest V_{OCV} for discharging case as well as the LIBs with the highest resistance are considered as the weakest. As an improvement to the used ECM shown in references above, its extended version is presented in Ref. [30] for SoAP prediction. For this reason, a second RC-element capturing diffusion processes is added to the basis ECM. A RLS filter is used for estimating the parameters of the diffusion branch. The proposed algorithm is verified under various conditions (various SoC ranges and different temperatures) by using real vehicle data. Unfortunately, no long-term robustness analysis of the proposed algorithm is performed.

3.2.2. Weighted recursive least square-based methods

In Refs. [81,82] the authors apply a direct differential (DD) algorithm to estimate battery states (SoC, SoAP and SoH) and the

WRLS algorithm to identify the impedance parameters of an R-$R_{ct}R_dC$ ECM. Diffusion resistance (R_d) is derived empirically and connected in series with charge transfer resistance (R_{ct}). According to the authors, considering the R_d in the ECM increases the SoAP prediction accuracy for discharge cases and for prediction time horizons in a range of $\Delta t \geq 10$ s significantly. However, the R_d is not implemented as an adaptive parameter in the proposed algorithm, and the fact that it changes over the battery lifetime and under different operating conditions [30] may lead to the decrease of the estimation accuracy over the battery lifetime.

In Refs. [83,90], the authors present an algorithm based on the WRLS technique for estimating the impedance parameters of an ECM that considers the mass transport effects by incorporating the Warburg impedance. Moreover, the current dependence of the R_{ct} is considered, and the applicability of the Tafel-equation for determining the R_{ct} in case of high current-rates is proven. The applied algorithm is verified under various conditions (different temperatures and different aging states of the battery) by investigating LIBs using NMC and LFP cathode materials. Based on the developed algorithm, battery V_{OCV} and SoC, respectively, are derived from an employed ECM by using the SoC-OCV correlation. Furthermore, the actual battery SoH using the estimated battery impedance and SoAP is determined on-board. However, for SoAP prediction the authors consider only the battery voltage as a limiting factor and determine the maximum current rate that the battery can deliver or accept.

3.3. Other adaptive filters and observer methods

In Ref. [86], the authors propose an SoAP estimation algorithm putting special emphasis on investigating time horizons much larger than in the researches presented above (i.e., $\Delta t \geq 60$ s). Asymmetric ECM parameters (R-RC-RC) for charge and discharge directions are considered in the applied algorithm. According to the authors, variation of the ECM parameters is necessary when SoAP prediction is performed for larger time horizons. The asymmetric parameter values yield higher estimation accuracy for appropriate charge and discharge directions. In this regard, two different SoAP prediction algorithms are investigated. First, a voltage limited-based method extrapolating battery resistances and V_{OCV} (so-called VLERO) is investigated. Second, a method based on a so-called multi-step model predictive iterative (MMPI) technique. Furthermore, battery SoC, voltage and current are considered as limiting factors for SoAP prediction. Applied algorithms are able to calculate the maximum battery current whereas voltage and SoC design limits are used. For verification reasons, the proposed algorithms are evaluated by means of the UDDS load profile at low temperatures (0 °C and −20 °C). According to the obtained results, the MMPI technique shows a higher degree of SoAP prediction accuracy. However, since the proposed algorithms are only evaluated under a MIL environment, it is recommended to examine their performance under real conditions as the next step.

Moreover, in Ref. [87] the authors propose a model-based approach using the Levenberg-Marquadt methodology for SoAP estimation in an example of a lithium-ion battery pack ($n_s = 20$, $n_p = 4$). The proposed technique is then compared with the technique based on the bisection methodology described in Ref. [76]. LIBs using NMC and LFP cathode materials are used to perform verification tests. The applied algorithm is evaluated by means of FUDS, dynamic stress test (DST) load profiles and HPPC tests. The authors investigate two R-RC ECMs where the first ECM neglects the V_{OCV} hysteresis and the second one uses a one-state hysteresis. Battery SoC, voltage and current are considered as limiting factors for SoAP prediction. According to the authors, the bisection technique shows some advantages over the proposed algorithm with

regard to its computational efficiency. However, the inconsistency of individual LIBs in the lithium-ion battery pack is neglected and it is assumed that the LIBs show a similar behavior. Moreover, battery nonlinearities are neglected.

In Ref. [21], a model-based approach for SoAP estimation in an example of a lithium-ion battery pack ($n_s = 16$, $n_p = 1$) for HEVs is discussed. In addition to the battery's voltage design limits, SoC and current limits are calculated and considered as further limiting factors for SoAP prediction. An R-RC ECM is employed and based on determined impedance parameters, the SoAP is predicted. However, the proposed SoAP prediction algorithm is verified under nominal conditions for LIBs in new state by comparing the results from HPPC test and DST load profile. The authors do not give information about the applied technique for on-board impedance parameters estimation. According to the results shown in this paper, the discussed theory with regard to the over and under estimation of the available battery power by means of the HPPC test in Section 1 is approved.

In Ref. [35], contrary to the above-mentioned approaches, the authors apply the particle filter (PF) technique for estimating the SoAP where battery SoC serves as an input parameter. The main advantage of PF-based techniques in comparison to other Bayesian filters is the possibility of approximating the probability density functions (PDF) even if non-Gaussian measurement uncertainty is given. A dependence of the polarization resistance on SoC and current ($R = \mathrm{f}(SoC, I)$) is used as a basis for an accurate instantaneous SoAP prediction. Thereafter, the Gaussian shape is chosen as membership function of the employed fuzzy set. The measured current and the voltage estimated from the employed ECM are used for the implemented PF algorithm. In the presented approach, the battery's SoC is firstly estimated based on the PF method, and the SoAP is determined by evaluating the resulting PDF function of the estimated SoC performed by means of a simple look-up table representing the relationship between SoAP and battery SoC. However, the authors use a simplified "fuzzy" ECM (ECM1 is responsible for charging case, ECM2 is responsible for discharging case) whereas the double-layer capacitance and the temperature's influence are neglected.

In Ref. [22], the impedance parameters of the employed ECM (R-RC) and battery SoAP are estimated based on a genetic algorithm. The presented approach is validated by means of the FUDS load profile for LIBs using the LFP cathode in a new state whereupon a lithium-ion battery pack ($n_s = 1$, $n_p = 9$) is used. The difference between both charge and discharge ohmic resistances (R_{dch}, R_{ch}) is considered in the employed ECM. In the first step, the authors apply a SOC-limited method for instantaneous SoAP prediction. Afterwards, a voltage-limited method is applied where the change of V_{OCV} over the prediction time horizon (Δt) is considered in order to improve the SoAP prediction accuracy. The obtained results compared with the results of the HPPC-based method discussed in Section 1 indicate a higher estimation accuracy of the proposed algorithm within an accuracy range of 2%.

3.4. Fuzzy logic and machine-learning-based methods

In addition to the techniques discussed above, there are some publications dealing with machine learning-based algorithms for SoAP prediction. The underlying idea of such techniques is based on the ability to learn and to adjust the relationship between input and output signals without the need of complex mathematical functions by using human knowledge. However, the development of machine learning based methods is still in a primitive stage and the applied techniques need to be further modified and verified under real conditions.

In Ref. [88], the authors investigate a technique based on the BP

Table 1
Referenced works based on equivalent circuit models for SoAP prediction.

Possible references	Employed ECM	Applied estimation technique	Current dependence of the charge transfer resistance is considered?
[57]	−	MSP	No
[80]	R-RC-$(C(z))$	RELS	No
[32,85]	R-$R(I)C$	VPA	Yes
[30]	R-$R(I)C$-RC	VPA, RLS	Yes
[28,76]	R	KF	No
[40,71]	R-RC	KF	No
[44]	R-RC	DEKF	No
[83,90]	R-$R(I)C$-$\underline{Z}_W$	WRLS	Yes
[65,77]	R-RC	AEKF	No
[26,73−75]	R-RC	EKF	No
[84]	R-RC	RLS and DMC	No
[78]	R-RC-$\underline{Z}_W$	Fractional Joint KF	No
[86]	R-RC-RC	a) VLERO, b) MMPI	No
[68,70]	R-RC	KF	Yes
[34]	R-RC	RLSF and AEKF	No
[21]	R-RC	−	No
[22]	R and R-RC	Genetic algorithm	No
[35]	R	Particle filter	Yes
[89,91]		ANFIS, ANFIS + REKF	
[88]	−	BP neural network	
[4]	R-RC	RLSF	No
[81,82]	R-$R_{ct}R_dC$	WRLS	No
[87]	R-RC	Levenberg-Marquadt	No

neural network training algorithm for SoAP prediction. The BP neural network algorithm is a forward, mono transmission multi-layers network including an input layer (containing 2 nodes), hidden layer (containing 4 nodes) and output layer (containing 1 node) network. It allows considering the nonlinear battery behavior without the need of high-level hardware. The basic idea of the proposed algorithm is simple: When the output vector does not meet the expected values, then the output error is transformed to input layer and distributed to units of hidden layers, respectively. Thereafter, the estimation error of each layer can be obtained. Based on the obtained estimation error, the weight of each neuron is adjusted until the output vector reaches the correct values. The proposed technique is verified under nominal conditions by means of offline simulations and constant discharging power profiles. Its applicability on real-time applications needs to be investigated in greater detail in the future.

In Ref. [89], the authors present a method using an adaptive neuro-fuzzy-inference system (ANFIS) for on-board SoAP prediction whereby the main focus lies on the battery voltage prognosis. The proposed approach combines the strengths of two common techniques, the artificial neuronal networks (ANN) and fuzzy inference system (FIS), in such a way that the battery parameters are adapted to the actual aging state. In this regard, according to the authors, a meaningful convergence of the parameters can be ensured. However, the authors neglect the battery current as further limiting factor for predicting the SoAP. The obtained Software-in-the-Loop (SIL) test results indicate high algorithm feasibility and estimation accuracy. For a pre-defined time horizon the battery voltage is predicted within a relative estimation accuracy of less than 1%. The implemented algorithm acts more as an SoF algorithm since the model output delivers an answer as to whether a power pulse can be performed or not. Furthermore, in Ref [91], the authors show results employing the same algorithm as before with the difference that the battery's SoC is also considered as an additional input parameter of the employed model. Battery SoC is determined by means of the robust extended Kalman filter (REKF).

The algorithms mentioned above and the respective literature sources for techniques based on equivalent circuit models are listed and compared in Table 1.

4. Conclusion

In this study, the available techniques for predicting the State-of-Available-Power in electric vehicles are reviewed. To this end, scientific articles, technical literature and available patents dealing with the aforementioned topic are analyzed and each individual method is thoroughly discussed. Special emphasis is put on elaborating the strengths and weaknesses of the discussed methods.

State-of-Available-Power refers to the amount of power that the battery can deliver to or accept from the vehicle powertrain. The available battery power is mainly limited by battery SoC, temperature, current and voltage. At the same time, the actual aging state of the battery influences the battery power capability significantly. The techniques that have up to now been applied for predicting the State-of-Available-Power can be classified into the following two groups: The first group is based on so-called adaptive characteristic maps; the second group, which up to now has received most attention, is based on equivalent circuit models.

Since the approaches based on equivalent circuit models are most likely not able to reproduce the occurring electrochemical processes in the battery precisely, their achieved estimation accuracy may not be sufficient for particular applications under specific operating conditions (e.g., at very low temperatures etc.). Therefore, as an alternative, advanced electrochemical battery models are preferred. Electrochemical battery models use complex mathematical equations and different approximations depicting processes in high details which yield higher estimation accuracy. However, high model fidelity is actually achieved at the expense of higher computational and parametrization effort. Unfortunately, up to now techniques based on electrochemical models have received little attention for the State-of-Available-Power prediction.

According to the current state of the art, it can be summarized that techniques based on equivalent circuit models are the dominating techniques for the prediction of State-of-Available-Power in battery management systems. But with increasing computational power of the micro-controllers implemented in BMS, a reasonable increase in the use of electrochemical model-based approaches is expected. The focus in the future may be put on improving the available techniques with regard to their robustness under varying conditions, such as wide temperature range including low temperatures and at different battery aging states.

Nomenclatures

AEKF	Adaptive extended Kalman filter
ANFIS	Adaptive neuro-fuzzy-inference system
BEV	Battery electric vehicle
BMS	Battery management system
BoL	Begin of Life
BSE	Battery state estimation
BVE	Butler-Volmer equation
CAN	Controller area network
CC-CV	Constant current-constant voltage
CDKF	Central difference Kalman filter
DAE	Differential algebraic equation
DEKF	Dual extended Kalman filter
DD	Direct differential
DMC	Dynamic Matrix Control
DVA	Differential voltage analysis
ECM	Equivalent circuit model
EES	Energy storage system
EoL	End of life
EKF	Extended Kalman filter
EMF	Electro motive force
EV	Electric vehicle
FUDRLS	Fast upper-diagonal recursive least square
FIS	Fuzzy inference system
HEV	Hybrid electric vehicle
HIL	Hardware-in-the-Loop
HV	High voltage
isoSPI	Isolated communications interface
KF	Kalman filter
LIB	Lithium-ion battery
LFP	Positive electrode active materials with a common formula $LiFePO_4$
LS	Least square
LTO	Negative electrode active materials with a common formula $Li_4Ti_5O_{12}$
LV	Low voltage
MA	Moving Average
MMPI	multi-step model predictive iterative;
MIL	Model-in-the-Loop
NEDC	New European Driving Cycle
NMC	Positive electrode active materials with a common formula of $Lix(NixMnyCoz)O2$
OCV	Open circuit voltage
PDE	Partial differential equation
PDF	Probability density function
PHEV	Plug-in hybrid electric vehicle
REKF	Robust extended Kalman filter
RLS	Recursive least square
RELS	Recursive extended least square
RLSF	Recursive least square with optimal forgetting factor
SoA	safe operating area
SPM	Single particle model
SoH	State-of-Health
SoC	State-of-Charge
SoF	State-of-Function
SoAP	State-of-Available Power
SPKF	Sigma point Kalman filter
UDDS	Urban dynamometer driving schedule
UKF	Unscented Kalman filter
WLS	Weighted least squares
WRLS	Weighted recursive least squares

References

[1] S. Goriparti, E. Miele, F.D. Angelis, E.D. Fabrizio, R.P. Zaccaria, C. Capiglia, Review on recent progress of nanostructured anode materials for Li-ion batteries, J. Power Sources 257 (0) (2014) 421—443.

[2] B. Scrosati, J. Garche, Tillmetz, Advances in Battery Technologies for Electric Vehicles, first ed., Woodhead Publishing, 2015. ISBN: 9781782423980.

[3] B. Scrosati, J. Garche, Lithium batteries: status, prospects and future, J. Power Sources 195 (9) (2010) 2419—2430.

[4] R. Xiong, H. He, F. Sun, K. Zhao, Online estimation of peak power capability of Li-ion batteries in electric vehicles by a hardware-in-loop approach, Energies 5 (0) (2012) 1455—1469.

[5] M. Root, The Tab Battery Book — an In-depth Guide to Construction, Design, and Use, The McGraw-Hill Companies, 2011. ISBN: 978-0-07-173991-7.

[6] X. Luo, J. Wang, M. Dooner, J. Clarke, Overview of current development in electrical energy storage technologies and the application potential in power system operation, Appl. Energy 137 (0) (2015) 511—536.

[7] L. Saw, Y. Ye, A. Tay, Electro-thermal analysis and integration issues of lithium ion battery for electric vehicles, Appl. Energy 131 (2014) 97—107.

[8] S.C. Mueller, P.G. Sandner, I.M. Welpe, Monitoring innovation in electrochemical energy storage technologies: a patent-based approach, Appl. Energy 137 (0) (2015) 537—544.

[9] Y. Zheng, X. Han, L. Lu, J. Li, M. Ouyang, Lithium ion battery pack power fade fault identification based on shannon entropy in electric vehicles, J. Power Sources 223 (0) (2013) 136—146.

[10] W. Waag, S. Käbitz, D.U. Sauer, Experimental investigation of the lithium-ion battery impedance characteristic at various conditions and aging states and its influence on the application, Appl. Energy 102 (0) (2013) 885—897.

[11] L.H. Saw, Y. Ye, A.A. Tay, Integration issues of lithium-ion battery into electric vehicles battery pack, J. Clean. Prod. 113 (0) (2015) 1032—1045.

[12] R.R. Richardson, P.T. Ireland, D.A. Howey, Battery internal temperature estimation by combined impedance and surface temperature measurement, J. Power Sources 265 (0) (2014) 254—261.

[13] J. Jiang, C. Zhang, Fundamentals and Applications of Lithium-ion Batteries in Electric Drive Vehicles, John Wiley & Sons, Inc, 2015. ISBN: 9781118414781.

[14] Y. Zou, X. Hu, H. Ma, S.E. Li, Combined state of charge and state of health estimation over lithium-ion battery cell cycle lifespan for electric vehicles, J. Power Sources 273 (0) (2015) 793—803.

[15] S.F. Schuster, M.J. Brand, P. Berg, M. Gleissenberger, A. Jossen, Lithium-ion cell-to-cell variation during battery electric vehicle operation, J. Power Sources 297 (2015) 242—251.

[16] S. Bhattacharya, P. Bauer, Requirements for charging of an electric vehicle system based on state of power (SoP) and state of energy (SoE), in: Power Electronics and Motion Control Conference (IPEMC), 2012 7th International, vol. 1, 2012, pp. 434—438.

[17] Battery Test Manual for Electric Vehicles, U.S. Department of Energy Vehicle Technologies Program, Revision 3, 2015.

[18] A. Farmann, W. Waag, D.U. Sauer, Application-specific electrical characterization of high power batteries with lithium titanate anodes for electric vehicles, Energy 112C (0) (2016) 294—306.

[19] B. Balagopal, M.Y. Chow, The state of the art approaches to estimate the state of health (SOH) and state of function (SOF) of lithium ion batteries, in: Industrial Informatics (INDIN), 2015 IEEE 13th International Conference on, 2015, pp. 1302—1307.

[20] M.A. Monema, K. Trad, N. Omar, O. Hegazy, B. Mantels, G. Mulder, P.V. den Bossche, J.V. Mierlo, Lithium-ion batteries: evaluation study of different charging methodologies based on aging process, Appl. Energy 152 (0) (2015) 143—155.

[21] Z. Cai-ping, Z. Cheng-ning, S. Sharkh, Estimation of real-time peak power capability of a traction battery pack used in an HeV, in: Power and Energy Engineering Conference (APPEEC), 2010 Asia-Pacific, 2010, pp. 1—6.

[22] F. Sun, R. Xiong, H. He, W. Li, J.E.E. Aussems, Model-based dynamic multi-parameter method for peak power estimation of lithium-ion batteries, Appl. Energy 96 (0) (2012) 378—386 (smart Grids).

[23] G.L. Plett, Extended Kalman filtering for battery management systems of LiPB-based HEV battery packs: Part 3. State and parameter estimation, J. Power Sources 134 (2) (2004) 277—292.

[24] J. Song, R. Anderson, D. Oliver, and S. Thompson, "System and method for managing a power source in a vehicle," Apr. 15 2014, US Patent 8,698,348.

[25] S. Saxena, C.L. Floch, J. MacDonald, S. Moura, Quantifying EV battery end-of-life through analysis of travel needs with vehicle powertrain models, J. Power Sources 282 (0) (2015) 265—276.

[26] J.H. Kim, S.J. Lee, J.M. Lee, B.H. Cho, A new direct current internal resistance and state of charge relationship for the li-ion battery pulse power estimation, in: Power Electronics, ICPE '07. 7th Internatonal Conference on, 2007.

[27] D. Robinson, "Power source estimation methods and apparatus," Aug. 26

2010, WO Patent App. PCT/US2010/023,827.

[28] G. Plett, "Method for calculating power capability of battery packs using advanced cell model predictive techniques," U.S. Patent 7,321,220 B2, Jan. 22, 2008.

[29] A. Farmann, W. Waag, A. Marongiu, D.U. Sauer, Critical review of on-board capacity estimation techniques for lithium-ion batteries in electric and hybrid electric vehicles, J. Power Sources 281 (0) (2015) 114–130.

[30] W. Waag, Adaptive Algorithms for Monitoring of Lithium-ion Batteries in Electrical Vehicles, Ph.D. dissertation, ISEA-RWTH Aachen University, 2014. ISBN: 978-3-8440-2976-5.

[31] W. Waag, C. Fleischer, D.U. Sauer, Critical review of the methods for monitoring of lithium-ion batteries in electric and hybrid vehicles, J. Power Sources 258 (0) (2014) 321–339.

[32] W. Waag, C. Fleischer, D.U. Sauer, Adaptive on-line prediction of the available power of lithium-ion batteries, J. Power Sources 242 (0) (2013) 548–559.

[33] O. Bohlen and M. Roscher, "Method for determining and/or predicting the maximum power capacity of a battery," May 6 2014, US Patent 8,718,988.

[34] R. Xiong, F. Sun, H. He, T.D. Nguyen, A data-driven adaptive state of charge and power capability joint estimator of lithium-ion polymer battery used in electric vehicles, Energy 63 (0) (2013) 295–308.

[35] C. Burgos-Mellado, M.E. Orchard, M. Kazerani, R. Cárdenas, D. Sáez, Particle-filtering-based estimation of maximum available power state in lithium-ion batteries, J. Appl. Energy 161 (0) (2016) 349–363.

[36] M. Berecibar, M. Garmendia, I. Gandiaga, J. Crego, I. Villarreal, State of health estimation algorithm of LiFePO₄ battery packs based on differential voltage curves for battery management system application, Energy 103 (2016) 784–796.

[37] J. Vetter, P. Novak, M. Wagner, C. Veit, K.-C. Möller, J. Besenhard, M. Winter, M. Wohlfahrt-Mehrens, C. Vogler, A. Hammouche, Ageing mechanisms in lithium-ion batteries, J. Power Sources 147 (0) (2005) 269–281.

[38] S. Nejad, D.T. Gladwin, D.A. Stone, Sensitivity of lumped parameter battery models to constituent parallel-RC element parameterisation error, in: IECON 2014-40th Annual Conference of the IEEE Industrial Electronics Society, Oct 2014, pp. 5660–5665.

[39] S. Nejad, D. Gladwin, D. Stone, A systematic review of lumped-parameter equivalent circuit models for real-time estimation of lithium-ion battery states, J. Power Sources 316 (2016) 183–196.

[40] W. Larry, J. Phillip, J. Kollmeyer, T.M. Jahns, R.D. Lorenz, Implementation of online battery state-of-power and state-of-function estimation in electric vehicle applications, Energy Convers. Congr. Expo. (ECCE) (2012) 1819–1826.

[41] E. Meissner, G. Richter, Battery monitoring and electrical energy management: precondition for future vehicle electric power systems, J. Power Sources 116 (12) (2003) 79–98.

[42] G. Richter, "Method and device for determining the state of function of an energy storage battery," U.S. Patent US 6,885,951 B2, 2005.

[43] S. Rezvanizaniani, D. Liu, Y. Chen, J. Lee, Review and recent advances in battery health monitoring and prognostics technologies for electric vehicle (EV) safety and mobility, J. Power Sources 256 (0) (2014) 110–124.

[44] L. Pei, C. Zhu, T. Wang, R. Lu, C. Chan, Online peak power prediction based on a parameter and state estimator for lithium-ion batteries in electric vehicles, Energy 66 (0) (2014) 766–778.

[45] A. Boehm and J. Weber, "Adaptives Verfahren zur bestimmung der maximal abgebaren oder aufnehmbaren leistung einer batterie," DE Patent WO 2011/095368 A1, Aug. 11, 2011, WO Patent App. PCT/EP2011/050,024.

[46] Battery Test Manual For Low-Energy Energy Storage System for Power-Assist Hybrid Electric Vehicles, U.S. Department of Energy Vehicle Technologies Program, April 2013.

[47] D. Kim and D. JUNG, "Method of estimating maximum output of battery for hybrid electric vehicle," Apr. 14 2009, US Patent 7,518,375.

[48] O. Bohlen, Impedance-based Battery Monitoring, Ph.D. dissertation, RWTH Aachen University, 2008. ISBN: 978-3-8322-7606-5.

[49] O. Bohlen, J.B. Gerschler, D.U. Sauer, Robust algorithms for a reliable battery diagnosis managing batteries in hybrid electric vehicles, EVS 22 (2006).

[50] C. Vacher, "Method for calculating the parameters of the power battery of an electric motor vehicle," Sep. 7 2004, US Patent 6,788,069.

[51] J.E.B. Randles, Kinetics of rapid electrode reactions, Discuss. Faraday Soc. 1 (1947) 11–19.

[52] S. Buller, Impedance-based Simulation Models for Energy Storage Devices in Advanced Automotive Power Systems, Ph.D. dissertation, Institute for Power Electronics and Electrical Drives, RWTH Aachen University, 2003. ISBN: 978-3-8322-1225-4.

[53] D. Linzen, Impedance-based Loss Calculation and Thermal Modeling of Electrochemical Energy Storage Devices for Design Considerations of Automotive Power Systems, Ph.D. dissertation, ISEA RWTH-Aachen, 2006. ISBN: 978-3-8322-5706-4.

[54] M. Ceraolo, New dynamical models of lead-acid batteries, Power Syst. IEEE Trans. 15 (4) (2000) 1184–1190.

[55] F.M. Gonzalez-Longatt, Circuit Based Battery Models: a Review, IEEE Proceedings, 2006.

[56] H. Zhang, M.-Y. Chow, Comprehensive dynamic battery modeling for PHEV applications, in: Power and Energy Society General Meeting, IEEE, 2010, pp. 1–6.

[57] X. Hu, S. Li, H. Peng, A comparative study of equivalent circuit models for li-ion batteries, J. Power Sources 198 (0) (2012) 359–367.

[58] J.P. schmidt, Verfahren zur Charakterisierung und Modellierung von Lithium-

[59] Ionen Zellen, Ph.D. dissertation, KIT, 2013. ISBN: 978-3-7315-0115-2.

[59] A. Farmann, W. Waag, D.U. Sauer, Adaptive approach for on-board impedance parameters and voltage estimation of lithium-ion batteries in electric vehicles, J. Power Sources 299 (2015) 176–188.

[60] T. Kim, Y. Wang, H. Fang, Z. Sahinoglu, T. Wada, S. Hara, W. Qiao, Model-based condition monitoring for lithium-ion batteries, J. Power Sources 295 (2015) 16–27.

[61] G. Plett, Dual and joint EKF for simultaneous SOC and SOH estimation, EVS 21 (2005).

[62] B. Fridholm, T. Wik, M. Nilsson, Robust recursive impedance estimation for automotive lithium-ion batteries, J. Power Sources 304 (2016) 33–41.

[63] M.S. Grewal, A.P. Andrews, Kalman Filtering: Theory and Practice Using MATLAB, John Wiley & Sons, Inc., 2001. ISBN: 0-471-39254-5.

[64] R.E. Kalman, A new approach to linear filtering and prediction problems, J. Fluids Eng. 82 (1) (1960) 35–45.

[65] R. Xiong, H. He, F. Sun, X. Liu, Z. Liu, Model-based state of charge and peak power capability joint estimation of lithium-ion battery in plug-in hybrid electric vehicles, J. Power Sources 229 (0) (2013) 159–169.

[66] W. Waag, C. Fleischer, D.U. Sauer, On-line estimation of lithium-ion battery impedance parameters using a novel varied-parameters approach, J. Power Sources 237 (0) (2013) 260–269.

[67] R. Xiong, X. Gong, C.C. Mi, F. Sun, A robust state-of-charge estimator for multiple types of lithium-ion batteries using adaptive extended Kalman filter, J. Power Sources 243 (0) (2013) 805–816.

[68] L. Juang, P. Kollmeyer, T. Jahns, R. Lorenz, Improved nonlinear model for electrode Voltage-current relationship for more consistent online battery system identification, Ind. Appl. IEEE Trans. (3) (2013) 1480–1488.

[69] J. Kowal, Spatially-resolved Impedance of Nonlinear Inhomogeneous Devices – Using the Example of Lead-acid Batteries, Ph.D. dissertation, ISEA-RWTH Aachen, 2010, 978-3-8322-9483-0.

[70] L. Juang, P. Kollmeyer, T. Jahns, R. Lorenz, Improved modeling of lithium-based batteries using temperature-dependent resistance and overpotential, in: Transportation Electrification Conference and Expo (ITEC), 2014, IEEE, June 2014, pp. 1–8.

[71] J. Song, R. Anderson, Y. Li, Y. Zhao, and X. Yang, "Method for determining a power capability of a battery," Jul. 12 2012, US Patent App. 12/987,190.

[72] G.L. Plett, Extended Kalman filtering for battery management systems of LiPB-based HEV battery packs: part 1. Background, J. Power Sources 134 (2) (2004) 252–261.

[73] R. Anderson, Y. Zhao, X. Wang, X.G. Yang, Y. Li, Real time battery power capability estimation, in: American Control Conference (ACC), 2012, June 2012, pp. 592–597.

[74] Y. Li and X. Wang, "Parameter and state limiting in model based battery control," Mar. 5 2015, US Patent App. 14/015,241.

[75] T. Lee, "Frequency based battery model parameter estimation," Sep. 15 2015, US Patent 9,132,745.

[76] G. Plett, High-performance battery-pack power estimation using a dynamic cell model, Veh. Technol. IEEE Trans. 53 (5) (2004) 1586–1593.

[77] F. Sun, R. Xiong, H. He, Estimation of state-of-charge and state-of-power capability of lithium-ion battery considering varying health conditions, J. Power Sources 259 (0) (2014) 166–176.

[78] X. Li, J. Sun, Z. Hu, R. Lu, C. Zhu, G. Wu, A new method of state of peak power capability prediction for Li-Ion battery, VPPC (2015) 1–5.

[79] D. Schroeder, Intelligente Verfahren; Identifikation und Regelung nichtlinearer Systeme, Springer, 2010. ISBN: 978-3-642-11397-0.

[80] T. Feng, L. Yang, X. Zhao, H. Zhang, J. Qiang, "Online identification of lithium-ion battery parameters based on an improved equivalent-circuit model and its implementation on battery state-of-power prediction, J. Power Sources 281 (0) (2015) 192–203.

[81] S. Wang, M. Verbrugge, J.S. Wang, P. Liu, Power prediction from a battery state estimator that incorporates diffusion resistance, J. Power Sources 214 (0) (2012) 399–406.

[82] S. Wang, M. Verbrugge, J.S. Wang, P. Liu, Multi-parameter battery state estimator based on the adaptive and direct solution of the governing differential equations, J. Power Sources 196 (20) (2011) 8735–8741.

[83] C. Fleischer, W. Waag, H.-M. Heyn, D.U. Sauer, On-line adaptive battery impedance parameter and state estimation considering physical principles in reduced order equivalent circuit battery models part 1. Requirements, critical review of methods and modeling, J. Power Sources (0) (2014) 276–291.

[84] L. Wang, Y. Cheng, J. Zou, Battery available power prediction of hybrid electric vehicle based on improved dynamic matrix control algorithms, J. Power Sources 261 (0) (2014) 337–347.

[85] W. Waag, C. Fleischer, and D. Sauer, "Method for determining model parameters of electrochemical energy storage of e.g. electric vehicle, involves defining parameter record variant as new reference dataset to describe battery model and to determine maximum power of storage," Jul. 17 2014, DE Patent App. DE201,310,000,572.

[86] P. Malysz, J. Ye, R. Gu, H. Yang, A. Emadi, Battery state-of-power peak current calculation and verification using an asymmetric parameter equivalent circuit model, Veh. Technol. IEEE Trans. PP (99) (2015) 1–1.

[87] X. Hu, R. Xiong, B. Egardt, Model-based dynamic power assessment of lithium-ion batteries considering different operating conditions, Ind. Inf. IEEE Trans. 10 (3) (Aug 2014) 1948–1959.

[88] W. Haiying, H. Zhonghua, H. Yu, L. Gechen, Power state prediction of battery based on BP neural network, in: 7th International Forum on, 2012, Strategic

Technology (IFOST), 2012.

[89] C. Fleischer, W. Waag, Z. Bai, D.U. Sauer, On-line self-learning time forward voltage prognosis for lithium-ion batteries using adaptive neuro-fuzzy inference system, J. Power Sources 243 (0) (2013) 728—749.

[90] C. Fleischer, W. Waag, H.-M. Heyn, D.U. Sauer, On-line adaptive battery impedance parameter and state estimation considering physical principles in reduced order equivalent circuit battery models part 2. Parameter and state estimation, J. Power Sources (0) (2014) 457—482.

[91] C. Fleischer, W. Waag, D.U. Sauer, Adaptive on-line State-of-Available-Power prediction of lithium-ion batteries, J. Power Electron. 13 (4) (2013).